# The Crohn's disease-associated *Escherichia coli* strain LF82 rely on SOS and stringent responses to survive, multiply and tolerate antibiotics within macrophages.

Gaëlle Demarre [1,2], Victoria Prudent [1], Hanna Schenk [3,6], Emilie Rousseau [1], Marie-Agnes Bringer [4, 5], Nicolas Barnich [5], Guy Tran Van Nhieu [1], Sylvie Rimsky [1], Silvia De Monte [3, 6] and Olivier Espéli [1,*].

Affiliations

[1] CIRB – Collège de France, CNRS-UMR724, INSERM U1050, PSL Research University, 11 place Marcelin Berthelot 75005 Paris, France.
[2] Inovarion, Paris, France
[3] Department of Evolutionary Theory, Max Planck Institute for Evolutionary Biology, Plön, Germany
[4] Centre des Sciences du Goût et de l'Alimentation, AgroSup Dijon, CNRS, INRA, Université Bourgogne Franche-Comté, F-21000 Dijon, France
[5] Microbes, Intestin, Inflammation et Susceptibilité de l'Hôte. UMR Inserm/ Université d'Auvergne U1071, USC INRA 2018
[6] Institut de Biologie de l'Ecole Normale Supérieure, Département de Biologie, Ecole Normale Supérieure, CNRS, INSERM, PSL Research University, Paris, France

* for correspondence: olivier.espeli@college-de-france.fr

**Abstract**

Adherent Invasive *Escherichia coli* (AIEC) strains recovered from Crohn's disease lesions survive and multiply within macrophages. A reference strain for this pathovar, AIEC LF82, forms microcolonies within phagolysosomes, an environment that prevents commensal *E. coli* multiplication. Little is known about the LF82 intracellular growth status, and signals leading to macrophage intra-vacuolar multiplication. We used single-cell analysis, genetic dissection and mathematical models to monitor the growth status and cell cycle regulation of intracellular LF82. We found that within macrophages, bacteria may replicate or undergo non-growing phenotypic switches. This switch results from stringent response firing immediately after uptake by macrophages or at later stages, following genotoxic damage and SOS induction during intracellular replication. Importantly, non-growers resist treatment with various antibiotics. Thus, intracellular challenges induce AIEC LF82 phenotypic heterogeneity and non-growing bacteria that could provide a reservoir for antibiotic-tolerant bacteria responsible for relapsing infections.

42 **Introduction**

43 Adherent Invasive *Escherichia coli* (AIEC) strains recovered from Crohn's disease (CD)
44 lesions are able to adhere to and invade cultured intestinal epithelial cells and to survive
45 and multiply within macrophages (Darfeuille-Michaud *et al*, 1998; Glasser *et al*, 2001).
46 Attention around the potential role of AIEC in the pathophysiology of CD is growing
47 (Elhenawy *et al*, 2018); however much remains to be learned about the host-pathogen
48 interactions that govern AIEC infection biology. The diversity of virulence factors
49 displayed by multiple AIEC strains suggests that members of this pathovar have evolved
50 different strategies to colonize their hosts (Tawfik *et al*, 2014). AIEC ability to persist,
51 and in some cases replicate within macrophages is particularly intriguing. Previous
52 work performed with murine macrophage cell lines has revealed that the prototype
53 AIEC strain LF82, multiplies in a vacuole presenting the characteristics of a mature
54 phagolysosome (Bringer *et al*, 2006; Lapaquette *et al*, 2012). In such an environment,
55 AIEC should encounter acidic, oxidative, genotoxic and proteic stresses. Screening of
56 genes involved in LF82 fitness within macrophage has revealed that HtrA, DsbA, or Fis
57 proteins are required for optimum fitness, (Bringer *et al.,* 2005; Bringer *et al.,* 2007;
58 Miquel *et al.,* 2010). These observations confirmed that LF82 encounter stresses in the
59 phagolysosomes. The impact of these stresses on the survival and growth of LF82 inside
60 phagolysomes has not yet been investigated.

61 Studies on the bacterial cell cycle of few model organisms under well-controlled
62 laboratory conditions have revealed that to achieve accurate transmission of the genetic
63 information and optimal growth of the population, molecular processes must be
64 coordinated. (for reviews see Hajduk *et al.,* 2016; Haeusser & Levin, 2008). When
65 growth conditions deteriorate, the cell cycle can be modified slightly, as in the case of
66 cell filamentation when genotoxic stress induces the SOS response, or more drastically
67 when sporulation is induced by nutrient deprivation (Jonas, 2014). Such cell cycle
68 alterations affect the entire population. However, under unperturbed conditions, a
69 subset of the population also appears to present a significantly reduced growth rate that
70 allows tolerance to antibiotic treatments. This small portion of the population, typically
71 1/10000 bacteria, is known as persisters (Wood *et al.,* 2013; Lewis, 2010; Bigger, 1944).
72 Persisters have been detected for a number of bacteria. They can be found
73 spontaneously in normally growing or stationary phase populations, or they are induced
74 by exogeneous stresses or mutations. Significant increase of the proportion of *S.*

75 *typhimurium* persisters has been observed when these bacteria invade macrophages
76 (Helaine *et al.,* 2014). Using a fluorescent reporter, it has been demonstrated that these
77 persisters were not multiplying prior to antibiotic addition. Recently, the same tool also
78 revealed the presence of non-growing mycobacteria inside macrophages (Mouton *et al.,*
79 2016). Several mediators of persistence have been identified, with toxin-antitoxin
80 modules emerging as key players and the reduction of metabolic activities as the main
81 driver of persistence (Rycroft *et al.,* 2018; Dörr *et al.,* 2009; Shan *et al.,* 2017; Balaban *et*
82 *al.,* 2004; Harms *et al.,* 2017; Amato *et al.,* 2014). Persisters are increasingly viewed as a
83 major cause of the recurrence of chronic infectious disease and could be an important
84 factor in the emergence of antibiotic resistance (Verstraeten *et al.,* 2016). In addition to
85 persisters, bacterial tolerance to antibiotic treatments has been observed. In contrast to
86 persisters, tolerance concerns the entire population. Tolerance corresponds to a weaker
87 ability of antibiotics to kill slow growing compared to fast growing bacteria. Tolerant
88 bacteria emerge, for example, in the presence of a nutritional limitation. The viability of
89 tolerant bacteria is impacted by the concentration and length of the antibiotic challenge
90 (Kim & Wood, 2017). Tolerant cells have some aspect of active metabolism, and their
91 frequency in the population changes when bacterial environmental sensing is altered
92 (Amato & Brynildsen, 2015; Bernier *et al.,* 2013; Radzikowski *et al.,* 2016). Persistence is
93 often viewed as the result of a phenotypic switch ensuring long-term adaptation to
94 variable environments, however the origin of persistence and tolerance *in vivo* remain
95 unclear, and their distinction in the context of a host- pathogen interaction is difficult
96 (Kim & Wood, 2017).
97
98 In the present work, we analyzed growth characteristics of the prototype AIEC strain
99 LF82 in THP1 monocyte–derived macrophages. We observed that stresses within
100 macrophages induce a profound bacterial response that leads to the formation of non-
101 growing and antibiotic-tolerant LF82 bacteria at a high rate through the successive
102 induction of stringent and SOS responses. A portion of non-growing LF82 produced
103 within macrophages is tolerant to antibiotics and presents a survival advantage. Our
104 work revealed that internalization within phagolysosomes curbs bacterial
105 multiplication, and frequent escape from the replicative cycle toward non-growing
106 state(s) is a way to improve long-term survival in the host.
107

108 **Results**

109

110 **Inside macrophages, LF82 population size increases despite extensive death.**

111 We used THP1 monocyte-derived into macrophages to monitor the population size of
112 LF82 bacteria over a 24 h period post infection (P.I.) (Figure 1A). Colony-forming units
113 (CFU) measurements revealed that the LF82 population exponentially increased for 10-
114 14 hours ($\tau$= 0.15 $h^{-1}$, 0.21 doubling / h) after a long lag. The population reached a
115 maximum at 18-20 h of approximately 5-fold the value at 1 h; the number of LF82 then
116 slightly decreased (reaching 3 -fold) at 24 h. In this environment LF82 might
117 simultaneously encounter acidic pH, oxidative and genotoxic stresses, toxic molecules
118 such as cathepsins and a lack of important nutrients. Surprisingly, the tolerance level of
119 LF82 to any individual stress did not differ from a K12-C600 *E. coli* in *in vitro* conditions
120 (Supplementary Figure S1A). Using direct ex vivo Live and Dead labeling, it has been
121 previously proposed that 80% of LF82 present at 24h within macrophages were alive
122 (Lapaquette *et al.,* 2012). We observed that this method slightly underestimates dead
123 bacteria inside macrophages because of a weak propidium iodide (PI) labeling
124 (Supplementary Figure S2A). Live and dead assay performed immediately after
125 macrophage lysis revealed a nearly constant proportion of dead LF82 in the population
126 (20 - 30%) at 1 h, 12 h, 18h and 24 h post-infection (Figure 1A). To estimate the speed of
127 dead bacteria disappearing in macrophages, we observed the elimination of heat-killed
128 bacteria by THP1 macrophages. Dead LF82 disappeared exponentially with a decay rate
129 of 0.6 $h^{-1}$ and a half-life of 1.4 h (Supplementary Figure S2B); therefore dead LF82
130 observed at 12h, 18h or 24 h did not correspond to the accumulation over infection
131 period but rather to the bacteria killed in the last 3 hours before observations. This
132 finding led to consider that LF82 must be under stress attack by macrophages at all
133 times during infection.

134

135 **LF82 is under attack by macrophages.**

136 Using RT-qPCR, we measured the expression of genes induced by the acid (*asr*, *ydeO* and
137 *frc*), oxidative (*soxS* and *ykgB*), and SOS (*sulA*) responses, and the responses to
138 membrane alteration (*pspB*), the lack of Mg2+ (*mgrB*), the lack of phosphate (*phoB*),
139 general efflux pump (*emrK*) and the *gltT* tRNA gene that is repressed by the stringent
140 response (Figure 1B). Every response pathway was induced inside the macrophage. The

141 induction of acid and the oxidative responses was already high at 1 h P.I., while the SOS
142 response, the response to membrane alterations and to the lack of Mg2+, were peaking
143 at 6 h P.I.. The expression of the *gltT* tRNA was strongly repressed at 1 h P.I. indicating
144 that stringent response is on early in the infection. The induction of most pathways
145 decreased at 24 h.
146
147 **Environmental stresses influence LF82 survival.**
148 To test the impact of stress responses on the ability of LF82 to colonize macrophage, we
149 constructed deletion mutants of several key regulators of *E. coli* stress pathways and
150 analyzed their survival. Deletion of the acid stress regulators *evgA-evgS*, *phoP* and *ydeO*
151 significantly impacted the ability of LF82 to survive and multiply within macrophages to
152 a level comparable to or even below that of a K12-C600 *E. coli* (Figure 1C). Similar
153 observations were obtained with the *rpoS* (general stress response), *recA* (SOS
154 response), *soxS* (oxidative stress) and *pspA* and *htrA* (envelope damages) deletion
155 mutants. The ppGpp0 strain, *relA spoT* deletions, impaired in the stringent response
156 reporting a lack of nutrients, is the most impacted strain; less than 5% of the initial
157 population survived a 24 h period within macrophages. These observations confirmed
158 that LF82 encounter severe stresses in the macrophage environment and that its ability
159 to repair stress mediated injuries will determine survival.
160
161 **SOS and stringent responses severely impacted LF82 survival**
162 Because of their known potential to influence growth and cell cycle parameters we
163 explored the stringent and SOS responses in more details. RecA is the main inducer of
164 the SOS response, which activates nearly 100 genes involved in DNA repair and many
165 others with unrelated or unknown functions, but it is also a crucial to correct DNA
166 lesions by homologous recombination and translesion synthesis (Kreuzer, 2013). In
167 addition to *recA* deletion, we constructed deletions of *sulA* (division inhibitor) and a
168 mutation in *lexA* (*lexAind-),* which blocks SOS induction in MG1655 *E. coli* and reduces
169 viability in the presence of mitomycin C for LF82 and MG1655 (Supplementary Figure
170 S3A). We observed that the deletion of each SOS gene significantly decreased the
171 survival of LF82 within macrophages (Figure 1C). Inside the macrophage, survival of the
172 ppGpp0 strain was dramatically impacted. However, this mutant also presented a strong
173 growth defect in liquid culture that complicates interpretation of the macrophage

174 results. To study the impact of the stringent response on LF82 survival and induced
175 antibiotic tolerance, we constructed deletion mutants that might have partial stringent
176 response phenotypes; deletion of *dksA,* encoding a protein linking the stringent
177 response to transcription (Sharma & Chatterji, 2010); and deletion of the polyphosphate
178 kinase and exopolyphosphatase *ppk* and *ppx* (Rao & Kornberg, 1999). As expected, the
179 *dksA and ppk-ppx* deletions had a much less dramatic effect on LF82 growth and
180 survival within macrophages than the *relA-spoT* mutant; nevertheless, the *dksA*
181 mutation significantly impacted the number of live bacteria recovered at 24 h P.I.
182 (Figure 1C). We investigated the ability of LF82 to survive within macrophages when
183 both stringent and SOS responses were altered. We chose to combine *dksA* deletion with
184 *recA* deletion or *lexAind-* mutation. These strains presented a survival defect comparable
185 to that of the single *dksA* mutant (Figure 1C). These observations demonstrate that
186 surviving LF82 simultaneously or successively require SOS and stringent responses.
187
188 **Inside phagolysosomes individual LF82 were not homogenously responding to**
189 **stresses.**
190 Imaging revealed great heterogeneity in the number of LF82 bacteria within individual
191 macrophages. At 18 h or 24 h P.I., many macrophages presented fewer than 5 bacteria,
192 which was comparable to the amount observed at 1 h P.I. (Figure 2A); however, a
193 number of macrophages also presented foci containing up to 50 bacteria (Figure 2B).
194 These observations led us to consider that LF82 were not homogeneously stressed by
195 macrophages. We used GFP fusion with selected stress response promoters to monitor
196 variability of these responses among bacteria and among macrophages (Figure 2B). For
197 all stress responses, heterogeneity in GFP fluorescence for intracellular bacteria was far
198 larger than for LB cultures (Figure 2 F - G). At 24 h P.I., we found that approximately
199 30% of the bacteria had poorly responded to oxidative or acid responses (Figure 2E and
200 2F). Owing the high stability of the GFP protein that we used in this assay, it is unlikely
201 that this heterogeneity resulted from short pulses of induction separated by long
202 repression periods. Such a sizeable phenotypic heterogeneity was moreover observed
203 for bacteria contained in a single macrophage as well as similar Lamp 1 positive
204 vacuolar environments (Figure 2C). We therefore questioned whether heterogeneity in
205 stress response might reflect the coexistence of multiple cell cycle regulation
206 phenotypes.

207

208 **Macrophages induce the formation of non-growing LF82**

209 We analyzed heterogeneity in LF82 cell cycle within macrophages by using two
210 complementary fluorescence assays. First, Fluorescent Dilution (FD) highlights bacteria
211 that have not divided since the time of infection (Figure 3A and Supplementary Figure
212 S4A-C).

213 FD shows that at 24 h P.I. LF82 underwent up to 6 divisions, which is still below the
214 maximum dilution detectable by the assay in our conditions (8 generations in LB,
215 Supplementary Figure S4B). In good agreement with the CFU, measurement of FD
216 showed that only 20% of the population has performed more than 1 division at 6 h P.I.
217 From these observations, we can estimate that the highest generation rate of LF82
218 within macrophages is ≈ 0.5 doubling /h between 6 and 20 h P.I.. Interestingly, FD also
219 revealed that approximately 4% of the population did not divide or divided fewer than 2
220 times intracellularly in 24 h (Figure 3A and Supplementary Figure S4B). By contrast
221 among the small amount of K12-C600 bacteria that survived for 24 h in the macrophage,
222 60% of K12-C600 bacteria underwent fewer than 2 divisions and less than 10%
223 underwent 5 divisions (Supplementary Figure S4D). Second, we used TIMER to refine
224 these observations; it provides an instantaneous evaluation of the generation time
225 during the infection kinetics (Figure 3B and S4A and S4B). TIMER indicated that at 18 h
226 P.I., 18% of the LF82 population was not actively dividing, supporting the existence of a
227 non-growing or slow-growing subpopulation. Since they require dilution of fluorescent
228 proteins both TIMER and FD are poorly informative about the first hours of the
229 infection. Therefore, we used a GFP fusion with the septal ring protein FtsZ to monitor
230 division in the individual bacterium (Figure 3C). In LB, exponentially growing LF82
231 frequently presented the FtsZ ring (70% of the population), but stationary phase LF82
232 rarely presented the FtsZ ring (<2% of the population, Figure 3D). Following infection of
233 macrophages with the stationary phase culture of LF82 *ftsZ-gfp*, we observed that 5%
234 (+/-2) and 40% (+/- 12) of the population, respectively, presented a FtsZ ring at 1 h and
235 24 h P.I. (Figure 3C and 3D). Following infection with exponentially growing LF82 we
236 observed a sudden reduction in the number of LF82 presenting a FtsZ ring at 1 h and 4h
237 P.I. (Figure 3D). The three reporters (FD, TIMER and FtsZ) provided complementary
238 indications: i) within macrophages, LF82 strongly slow down their cell cycle for several
239 hours; ii) starting at 6 h P.I. LF82 multiply; in this phase the generation time may vary

240 among bacteria but can be as short as 2h; iii) a part of the population, completely halted
241 their cell cycle and become non-grower. The difference between the number of non-
242 growing LF82 revealed by TIMER and FD shows that non-growing LF82 are formed late
243 in the infection kinetics and not only upon phagocytosis.
244
245 **Macrophages induce the formation of antibiotic-tolerant LF82.**
246 Non-growing Salmonella phenotypes have been observed inside macrophages and
247 during mouse infection (Helaine *et al.,* 2014; Claudi *et al.,* 2014). Being tolerant to
248 subsequent antibiotic challenge they were recognized as persisters. We inquired
249 whether also for AIEC LF82 the non-growing component of the population had
250 enhanced antibiotic tolerance. In exponentially growing liquid cultures, approximately
251 0.01% LF82 tolerated a 3 h ciprofloxacin challenge, and can therefore be considered
252 persisters (Figure 4A). Following a brief passage through the macrophage, the frequency
253 of LF82 bacteria tolerant to ciprofloxacin increased to 0.5 % (nearly 50 fold compared to
254 exponentially growing LF82). Interestingly the number of tolerant LF82 reached 5%
255 (500 fold compared exponentially growing LF82) after 24 h in the macrophage (Figure
256 4A). This near to 10-fold increase in the number of tolerant bacteria after a 24 h
257 intracellular period compared to a 1 h intracellular period indicates that, like non-
258 growers, tolerant phenotypes are not exclusively formed upon infection, but also as
259 bacteria multiply inside the macrophage. In this respect, the behavior of LF82 differs
260 significantly from *S. typhimurium*, which forms a large number of persisters upon
261 macrophage entry , but this population remains stable during the infection (Helaine *et*
262 *al.,* 2014). To test if non-growing LF82 revealed by the FD assay indeed corresponded to
263 the antibiotic-tolerant population, we used the macrophage-permeable antibiotic
264 ofloxacin. We added ofloxacin (10x MIC) for 4 h after 20 h of intracellular growth, and
265 we observed significant increases in the proportion of green LF82 (non-growing) inside
266 macrophages (Figure 4B). These observations suggest that the sub-population of non-
267 growing bacteria largely overlaps with that of persisters, where protection from
268 antibiotics may also confer enhanced tolerance to intracellular stresses.
269
270 **Tolerance to antibiotics is enhanced for LF82 compared with K12-C600 *E. coli.***
271 We compared the number of LF82 and a non-pathogenic K12-C600 laboratory strain
272 with tolerance to ciprofloxacin following brief (1 h) or long (24 h) passages in

273 macrophages. After a brief passage in macrophages, the proportion of LF82 that were
274 tolerant to ciprofloxacin was significantly higher for LF82 than K12-C600 (Figure 4C).
275 Interestingly, even if the absolute number of ciprofloxacin-tolerant K12-C600 was
276 largely reduced compared with LF82, their proportions among bacteria that survived 24
277 h inside macrophages were comparable (Figure 4C). These findings demonstrate that
278 the number of antibiotic-tolerant bacteria formed in response to macrophage attack is
279 reinforced for LF82 compared with the laboratory strain.
280
281 **Tolerance to antibiotics is a transient state.**
282 We next evaluated whether the antibiotic tolerance was a stable or transient phenotype.
283 We used the macrophage lysis procedure to recover LF82 with induced persistence for 1
284 h in the macrophage; then, we either challenged them immediately with ciprofloxacin or
285 allowed them to recover in LB for 1 h or 2 h before antibiotic challenge. When bacteria
286 were cultured for 1 h in LB, the frequency of tolerant bacteria was decreased in
287 comparison to bacteria that were immediately treated with the antibiotic; however, this
288 number was still higher than that of bacteria that had not infected macrophages. Two
289 hours in LB was sufficient to cause a comparable frequency of ciprofloxacin-tolerant
290 LF82 to that of bacteria that had not encountered macrophages (Figure 4D). These
291 observations show that when the environment is no longer stressful, antibiotic-tolerant,
292 non-growing LF82 rapidly switch back to a replicative mode.
293
294
295 **Characterization of non-growing LF82.**
296 Both FD and TIMER revealed slightly more non growing LF82 (4% and 18%
297 respectively, figure 3A) than antibiotic-tolerant LF82 after macrophage lysis (0.5% at 1
298 h P.I. or 5% at 24 h P.I. , Figure 4A). This finding raised the possibility that persisters
299 only form a portion of the non-growing population. To quantify this proportion, we
300 infected macrophages with TIMER-tagged LF82, lysed the macrophages and allowed
301 bacterial growth on a LB-agarose pad under the microscope at 37°C. Seventy percent of
302 the LF82 bacteria recovered quickly from the challenge and formed microcolonies, but
303 approximately 30% of them never divided (Figure 4E). These non-cultivable LF82
304 presented either non-growing or growing TIMER fluorescence (Figure 4F). The presence

305 of non-cultivable LF82 among the bacteria with non-growing TIMER fluorescence
306 explains the difference between fluorescence and antibiotic assays.
307
308 **SOS and stringent responses influence antibiotic tolerance.**
309 Among mutants that affected LF82 survival (Figure 1C), only the *recA*, *relA spot* and *dksA*
310 deletions negatively impacted the number of LF82 that were tolerant to a 3h
311 ciprofloxacin treatment (Figure 5A). The impact of the *recA* deletion might be
312 misinterpreted because ciprofloxacin alters DNA and limits resuscitation of *recA*
313 persisters. Therefore, we repeated the tolerance assay with cefotaxime for the following
314 SOS mutants: *recA* (impaired for DNA lesion repair and SOS induction), *lexAind-* (unable
315 to induce SOS) and *sulA* (unable to block cell division). I*n vitro*, SOS mutants did not
316 present defect for cefotaxime tolerance (Supplementary Figure S3B). However, these
317 mutants exhibited a decreased tolerance to antibiotics when persisters were induced by
318 a pretreatment with subinhibitory concentrations of ciprofloxacin (Supplementary
319 Figure S3C). This finding is in good agreement with previous reports (Dörr *et al.,* 2009),
320 and it confirms that SOS induction favors the production of persisters. We analyzed
321 cefotaxime tolerance of these SOS mutants after a 1 h or 20 h period within
322 macrophages (Figure 5B and 5C). We observed a significant reduction of the proportion
323 of *recA* and *sulA* mutants that were tolerant to cefotaxime treatment after a 20 h passage
324 in the macrophage (Figure 5C) but no effect on bacteria that remained only 1 h in
325 macrophages (Figure 5B). The *lexAind-* mutation did not change the number of tolerant
326 bacteria in these conditions. We also analyzed the *dksA* mutant in these assays;
327 surprisingly, it behaved differently than the *recA* and *sulA* mutants: we observed a
328 significant reduction of the proportion of cefotaxime tolerant bacteria following a 1 h
329 passage within macrophages (Figure 5B) but not when the bacteria remained for 20 h in
330 macrophages (Figure 5C). To test an eventual epistatic relation between SOS and
331 stringent response we combined *recA* and *dksA* deletions. They had an additive impact
332 on the ability of LF82 to become tolerant to cefotaxime after a brief infection (Figure 5B)
333 and a 20-hour infection (Figure 5C). Our observations suggest that production of
334 persister/tolerant LF82 bacteria is under the control of the stringent response in the
335 first hours of infection and controlled by genotoxic stress, the SOS response and DNA
336 lesion processing later in the infection. When one of these two responses is deficient the
337 production of persister /tolerant LF82 requires the other.

338

339 **The role of SOS response and stringent response for the control of LF82 cell cycle**
340 **in the macrophages.**

341 Knowing that SOS and stringent responses influence the production of antibiotic
342 tolerant LF82 after a passage within macrophage we examined whether they also
343 contributed to LF82 cell cycle control, i.e. production of non-growing, replicative or dead
344 LF82. We used the FD assay to measure the number of non-growing LF82 in *the relA-*
345 *spoT* and *recA* mutants. FD revealed that the non-grower number was dramatically
346 reduced in the *relA-spoT* mutant (<1%) (Figure 5D). This suggests that in the absence of
347 stringent response LF82 cannot immediately curb its cell cycle upon phagocytosis. By
348 contrast the number of non-growers was unchanged for the *recA* mutant (Figure 5E).
349 This is in agreement with the absence of effect of the *recA* deletion on the production of
350 cefotaxime tolerant LF82 early in the infections. TIMER revealed that at 20 h P.I. the
351 proportion of slow, mid and fast growing LF82 was affected by the alteration of *recA,*
352 *lexAind-, sulA* and *dksA.* The *recA* and *dksA* deletions reduced the number of non-growing
353 LF82; by contrast, the *lexAind-* and *sulA* mutations only increased the number of fast
354 growing LF82 in the population (Figure 5F). Finally, the live and dead assay showed a
355 strong increase in lethality of the *recA, sulA*, *lexAind-,relA spoT* and *dksA* mutants at both
356 time points (Figure 5G) suggesting that in the macrophage environment a failing cell
357 cycle control will almost certainly lead to LF82 death.

358 Altogether our results showed that the stringent response is the main controller of the
359 early intracellular survival of LF82; it limits LF82 growth and induces the formation of
360 non-growers and among them persisters. Later on, when replication is resumed, SOS
361 response grows in importance. DNA lesions that have been accumulated in the lag phase
362 must be repaired to allow replication and formation of new non-growers and new
363 persisters.

364

365 **Kinetics of macrophage infection**

366 AIEC LF82 tolerates macrophage induced stresses, thus it survives and multiplies in the
367 phagolysosome. The population expansion is accompanied by a rise in the number of
368 bacteria that do not grow and tolerate an antibiotic challenge (called henceforth
369 persisters). The change in time, during macrophage infection, of LF82 population size
370 and fraction of persisters are relevant to future fundamental studies, but also to devising

371 therapeutic strategies involving AIEC or other intracellular pathogens. In order to
372 explore the mechanistic bases of the infection kinetics, we have used a mathematical
373 model (Figure 6A) to fit the observed changes in CFU and persister counts during 24 h
374 for LF82, K12-C600 and the stringent response mutant LF82*dksA* (Figure 6B). The
375 model is based on the following biologically-informed hypotheses (illustrated in Figure
376 6A and detailed in the Supplementary text 1). i) Reproduction: the population of
377 replicating bacteria B has a constant net growth rate (birth minus death rate) $\delta_1$, which
378 is either 0 or negative during a lag phase of duration $\lambda$, and $\beta>0$ otherwise. ii) A stress-
379 induced death rate, $\delta_2(S)$ that increases with stress (S). We assume that stress S, possibly
380 due to lesions (DNA lesions, membrane alterations, oxidative damages among others)
381 that accumulate over time or due to a macrophage response to the infection, builds up in
382 time proportionally to the total number of bacteria in the population. iii) Switch to
383 persistence: bacteria have a constant probability $k_p$ of generating non-growing, stress-
384 tolerant phenotypes P. The dynamics of a population of bacteria can be described by a
385 set of three ordinary differential equations for the number B of non-persister bacteria,
386 the number P of persisters, and the stress variable S (Methods). The number of dead
387 bacteria D can be derived from these under the assumption that dead LF82 bacteria
388 decay exponentially with rate 0.56 (computed from the assay in Supplementary Figure
389 2C). The model has a total of 12 parameters for the three strains, which are fitted to data
390 as explained in Methods and SI. Although LF82 displays a considerable overshoot in
391 population size (as also observed in (Glasser *et al*, 2001)), the dynamics can be
392 reproduced by choosing the same $\beta$ for every strain. We estimated such net growth rate
393 to $0.15 \pm 0.003\ h^{-1}$, corresponding to 0.21 divisions per hour (Figure 6B), consistent with
394 independent cell-level measures by FD (Supplementary Figure 4). The most notable
395 quantitative difference between strains is that K12-C600 displayed a lag phase of more
396 than 13 h, twice as long as LF82 and LF82*dksA*. A consequence of this difference is that
397 when K12-C600 bacteria start actively duplicating, stress has already built up. Together
398 with K12-C600's enhanced sensitivity to stress, this curbs the population expansion,
399 resulting in a lower overall growth within macrophages. In the LF82*dksA* mutant,
400 growth is instead impaired by increased initial mortality (whose rate $\delta_1$ has been
401 estimated by PI measures, Supplementary Figure S2C), presumably related to stringent
402 response failure. With respect to the other strains, moreover, LF82 is advantaged at
403 later times – when the SOS response becomes important – thanks to reduced stress-

404 induced death rate. Rate of persistence production for LF82 and LF82 *dksA* (0.08 and
405 0.002 $h^{-1}$, respectively) is estimated to be higher than for K12-C600 (0.001 $h^{-1}$) ,
406 supporting the notion that AIEC strains within macrophages turn to persisters at an
407 enhanced rate, but less so if their stringent response is impaired. The model allows
408 testing changes in infection dynamics for 'virtual mutants' LF82*, obtained by varying $k_p$,
409 $\lambda$ and $d_{max}$ – the parameters that quantitatively differ between LF82 and *E. coli* K12-C600
410 (Figure 6C). The total population overshoot is enhanced when lag phase is shorter and
411 the effect of stress less acute, but damped when persisters production is more frequent.
412 Interestingly, the phenotypes of the single stress response mutants (acid, oxidative, lack
413 of $Mg^{2+}$), i.e. reduced CFU at 24 h without perturbation of the persister proportion in the
414 population (Figure 1C and 3A) were nicely reproduced by a change in the single $d_{max}$
415 parameter. This suggests that the model can be used to plan future works on the effect
416 of mutants or drugs on macrophage colonization by AIEC.
417
418
419 **Discussion**
420 We analyzed the growth and survival strategies used by the prototype AIEC strain LF82
421 to colonize the human monocytes-derived THP1 macrophages. Our analysis revealed
422 that intracellular LF82 are constantly under stress while colonizing macrophages. The
423 consequences of these stresses are important: increase in the death rate of bacteria,
424 slow multiplication of replicating bacteria and formation of a large number of non-
425 growing bacteria. LF82 adapts to this environment thanks to successive phenotypic
426 switches that require the two main stress responses: the SOS response and the stringent
427 response (Figure 7).
428
429 **Macrophages place LF82 under lethal stress.**
430 Using fluorescent reporters, we measured that half of the LF82 population present at 24
431 h P.I. had given rise to 6 or more generations. Under controlled laboratory conditions,
432 this should produce a 30 to 60-fold increase in the population size at 20 h compared
433 with the 1 h time point PI. However, we only observed a 3 to 6-fold increase in viable
434 bacteria at 20-24 h compared with 1 h. We demonstrated that this modest colonization
435 of macrophages by LF82 is explained by a big death rate and switch from replicative to
436 non-growing cell cycle. At the single-macrophage and single-bacterium level, FD and

437 TIMER fluorescent reporters revealed non-growing LF82. We observed macrophages
438 containing few (less than 4) LF82 with red fluorescent dilution staining. These bacteria
439 had therefore divided several times (>4) before observation and thus should be
440 accompanied by their siblings (>16). This observation is in good agreement with our
441 Live and Dead assay indicating that LF82 progeny has a significant chance to be killed
442 and destroyed by the macrophage. By contrast, some macrophages contained growing
443 LF82 and ultimately acquired more than 50 bacteria in one or several compartments.
444 The live and dead assay confirmed that LF82 was frequently killed by macrophages.
445 Because alterations of bacterial stress responses significantly reduced the bacterial
446 yield, we propose that LF82 death is the consequence of oxidative, acid, genotoxic and
447 protein stresses imposed by the macrophage. We compounded these experimental
448 observations in a mathematical model describing the dynamics of bacterial infection
449 within macrophages. A first phase of stalled growth, a likely combined effect of a
450 prolonged lag phase and of compensation between death and division, is followed by an
451 exponential increase in bacterial concentration. This second phase might correlate with
452 a transient increased permissiveness of phagolysosomes or more likely the adaptation
453 of LF82 to growth in this stressful environment. This expansion is successively curbed
454 by the building-up of stressors. Many persisters are formed in the first phase. However,
455 in the second phase a phenotypic switch to non-growing LF82 will eventually result in a
456 sizeable increase of the persister population. We thus understand the survival of LF82 as
457 a consequence of its ability to adapt to harsh phagolysosome environment both at the
458 entry of the macrophage, by induction of stress responses and particularly the stringent
459 response, and during exponential expansion by SOS response. LF82 advantage over K12-
460 C600 would reside in its ability to exit from the lag phase to perform a few rounds of
461 replication/division before stress becomes too strong (Figure 6). Strategically, early
462 onset of growth is compensated by production of persistent bacteria, which endows the
463 pathogenic strain with long-term survival in spite of rapid exploitation of the
464 macrophage environment. We have not yet identified LF82 specific regulons, genes or
465 mutations that allow this transition to take place.
466
467 **Replicative LF82.**
468 Fluorescent dilution revealed that after the exit of lag phase LF82 replicated moderately
469 within macrophages, with generation time longer than 2 h. *In vitro*, this would be

470 comparable with generation times observed in minimal medium with poor carbon
471 sources such as acetate. Our observations revealed that within macrophages, 40% of the
472 LF82 population presented an FtsZ ring, which is significantly above the number
473 expected from a mixed population of *E. coli* growing with a 2h generation time (28% of
474 cells with FtsZ ring (den Blaauwen *et al*, 2001)) and non-growing cells. Interestingly, in
475 spite of SulA induction, we did not observe filamentation of LF82 within macrophage.
476 These finding demonstrates that some of the cell cycle rules that were established under
477 defined *in vitro* conditions do not apply to intracellular growth conditions, opening
478 avenues for future investigations of bacterial cell cycle regulation in the context of host
479 infection or the microbiota.
480
481 **Non-replicative LF82.**
482 FD and TIMER revealed that a significant number of intracellular LF82 were not
483 growing. FD revealed that approximately 4% of the phagocytosed LF82 immediately
484 halted their cell cycle. TIMER revealed that at 20 h P.I., approximately 20% of the LF82
485 population was not growing. We also demonstrated that once the macrophages were
486 lysed, a large portion of the LF82 population (from 0.3 to 10%) was tolerant to several
487 hours of antibiotic challenge, and the proportion of non-growers in the population
488 increased in macrophages in the presence of antibiotics. Altogether, these observations
489 suggest that the phagolysosome environment induces frequent cell cycle arrests among
490 the population and that a part of this arrested population is persisters or tolerant to
491 antibiotics. Such a phenomenon has been previously described during *S. typhimurium*
492 infection of macrophages (Helaine *et al.,* 2014) or mice (Helaine *et al.,* 2014; Claudi *et al.,*
493 2014) and is reminiscent of VBNR mycobacteria (Manina *et al.,* 2015). Interestingly, we
494 observed an increase in the proportion of macrophage-induced antibiotic-tolerant LF82
495 at later time points, suggesting adaptive responses to the intracellular
496 microenvironment.
497
498 **Stress responses are important for LF82 survival within macrophages.**
499 As expected for bacteria residing in a toxic environment, stress responses are important
500 for LF82 survival within macrophages. Acidic, oxidative, genotoxic, and envelope
501 alterations, lack of Mg2+ and lack of nutrient stress responses significantly decreased
502 the fitness of LF82 (50 to 10% of WT). In a few cases, we demonstrated an additive

503 effect of simultaneously altering two pathways. However, LF82 demonstrated
504 surprisingly good tolerance to these alterations compared with the *in vitro* findings for
505 individual stresses. For example, *recA* deletion mutant was extremely sensitive (<1%
506 survival) to prolonged treatment with genotoxic drugs (Supplementary Figure S3A); by
507 comparison, in macrophages, despite clear SOS induction, the viability of the *recA*
508 mutant was only reduced by half compared with wild type bacteria. Set aside the
509 possibility that stress-less niches exist due a possible heterogeneity in the macrophage
510 population, the fitness decline of LF82 stress mutants may be limited by a combination
511 of slow growth, formation of non-growers and/or yet uncharacterized adaptation
512 pathways.
513
514 **SOS and stringent responses successively control LF82 fate.**
515 We investigated the trigger that could allow some LF82 to halt their cell cycle inside
516 macrophages. It appeared to be unrelated to the ability to sense acidic or oxidative
517 stress . At an early time point, stringent response mutants altered the survival and
518 production of antibiotic-tolerant LF82 suggesting that abrupt nutrient starvation is one
519 of the first signals received by LF82 upon phagocytosis. The early stringent response
520 should result in a slowdown of transcription, translation and DNA replication, and
521 therefore, it might provoke the formation of non-growers and a 7-h lag phase . We
522 assessed whether the stringent response impaired the declines in viability in this first
523 period, and we observed a decrease in the number of bacteria with undiluted GFP using
524 the FD assay, as well as a reduction in antibiotic-tolerant LF82 induction. This suggests
525 that the slowing down induced by the stringent response confers a temporary
526 protection than can be extended to antibiotic tolerance when bacteria become
527 persisters. Accordingly the impact of stringent response alteration was less apparent
528 after the lag phase when replication is re-established in a portion of the population of
529 LF82. SOS induction was moderate at 1 h but important at 6 h and 24 h P.I.; this is in
530 good agreement with the lack of an effect of *recA* deletion on the accumulation of LF82
531 with undiluted FD GFP and the lack of an influence of SOS mutants on the number of
532 LF82 that were tolerant to cefotaxim at 1 h after infection. DNA lesions could, however,
533 form during this period, but they were mostly observed when DNA replication restarted
534 after 6 h. In this second phase of infection, SOS induction in replicative bacteria might
535 play several roles: i) sustaining DNA repair and therefore DNA replication, cell division

536 and increases in population size; ii) decelerating the division progression, this is the role
537 of SulA, and thus contributing to the formation of new non-growers ; iii) intervening for
538 resuscitation of non-growers presenting DNA lesions, both within macrophages and
539 after macrophage lysis.
540
541 **Macrophages as a niche for LF82 survival**
542 The purpose of macrophage colonization by LF82 in Crohn's disease patients is not yet
543 understood. *In vitro*, LF82 colonization did not provoke extensive death of macrophages,
544 which are thus unlikely to serve as a transient replicative niche for ileal infection.
545 Alternatively, we can imagine that dormant LF82 within macrophages can serve as a
546 long-term storage. In this environment, bacteria might be protected from competition
547 with other species of the microbiota and coincidentally from antibiotics. Upon
548 macrophage lysis or inactivation, dormant LF82 would be released and would start to
549 multiply under adequate conditions.
550
551 **Methods**
552 **Strains and plasmids**
553 Deletion mutants (Supplementary Table S1) were constructed using the recombineering
554 method as described in (Demarre *et al.,* 2017). Plasmids are described in Supplementary
555 Table S2.
556
557 **Infection and microscopy**
558 THP1 monocytes ($5x10^5$ cells/ml) differentiated into macrophages for 18 h in phorbol
559 12-myristate 13-acetate (PMA, 20 ng/ml) were infected and imaged as previously
560 described (Demarre *et al.,* 2017). Infections were performed at MOI 30 (measured by
561 CFU), resulting in the observation of 3 LF82 bacteria per macrophage on average at 1 h
562 P.I.. Imaging was performed on an inverted Zeiss Axio Imager with a spinning disk CSU
563 W1 (Yokogawa).
564
565
566 **Antibiotic challenge and viable bacterial count using the gentamycin protection**
567 **assay**

568 To determine the number of intracellular bacteria after 20 min of infection, infected
569 macrophages were washed twice with PBS, and fresh cell culture medium containing 20
570 μg $ml^{-1}$ of gentamicin (Gm) was added for the indicated time (1 h to 30 h). Cell
571 monolayers were washed once with PBS, and 0.5 ml of 1% Triton X-100 in 1x PBS was
572 added to each well for 5 min to lyse eukaryotic cells (Bringer *et al.,* 2006). Samples were
573 mixed, diluted and plated on LB agar plates to determine the number of colony-forming
574 units (CFU) recovered from the lysed monolayers. For the antibiotic tolerance assays,
575 macrophage lysates were transferred to 5-ml tubes and centrifuged for 10 min at 4100
576 g. The pellet was either suspended in 1x PBS (t0) and ciprofloxacin (1 μg/ml) for 1 h and
577 3 h, or in LB and cefotaxim (100 μg/ml) for 1 h and 3 h. CFU were measured by serial
578 dilution. Tolerance was estimated for the 1-h and 3-h time points as a function of the
579 CFU at t0.
580
581 **Live and dead assay**
582 At the indicated time points, macrophages were lysed with vigorous resuspension in 1x
583 PBS 1% Triton. The cell lysate was pelleted at 300 g for 10 min to eliminate large cell
584 remnants. The supernatant was centrifuged at 4000 g for 10 min. The bacterial pellet
585 was suspended in 1x PBS and processed with the Live and Dead BacLight Viability kit
586 (Thermo Fisher). The bacteria were pelleted for 3 min at 5000 g, resuspended in 50 μl of
587 1x PBS and spread on a 1% agarose 1x PBS pad for immediate observation.
588
589 **Measurement of gene expression by RT-qPCR**
590 Total RNA was extracted with TRIzol reagent from $10^6$ macrophages, as described in the
591 *Molecular Cloning, a laboratory Manual* (Green and Sambrook, CSH Press). First-strand
592 cDNA synthesis was performed with the Maxima First Strand cDNA Synthesis Kit for RT-
593 qPCR (Thermo Fisher), and real-time qPCR was performed with SYBR Green Master Mix
594 (Bio-Rad) on a MyiQ real-time qPCR machine (Bio-Rad).
595
596 **Fluorescence quantification**
597 Custom-made FIJI macros were developed for the analyses of fluorescence. For the
598 Biosensors and FD, constitutive expression of mCherry from p-mCherry was used to
599 construct bacterial masks, which were subsequently used to measure GFP intensity. For

TIMER analyses, green fluorescence was used to construct the mask. Fluorescence distributions were analyzed with the distribution fitting tool in MATLAB.

**Mathematical model for the infection kinetics**

A set of three ODEs recapitulates the main features of the observed growth within macrophages, as explained in the main text and in the SI:

$$\frac{dB}{dt} = [1 - I(t < \lambda)]\beta B - k_p B - I(t < \lambda)\delta_1 B - \delta_2(S)B$$
$$\frac{dP}{dt} = k_p B \quad (1)$$
$$\frac{dS}{dt} = B + P$$

Here, $I(t < \lambda)$ is the indicator function, which is unitary during lag phase. At the beginning of the infection, thus, the net growth rate -$\delta_1$ is either zero (K12-C600 and LF82) or negative (stringent response mutant LF82dskA). At later times, net growth rate $\beta$ is instead positive. The stress-induced death rate has been chosen to be a sigmoidal function of the stress level:

$$\delta_2(S) = \frac{d_{max}}{1+e^{a(S-S_{1/2})}}$$

where the half-saturation stress value $S_{1/2}$ and the sensitivity parameter a are assumed to be identical for all strains. Here stress is an effective variable quantifying the effect of crowding on growth within macrophages, and could correspond both to density-dependent reduction of bacterial growth rate (e.g. due to resource depletion), and to the progressive buildup of macrophage-induced killing.

**Fit of the infection kinetics data**

Parameters providing the best fit of eqs. (1) to the times series of CFUs and persisters have been obtained by a weighted least-square distance minimization using the python differential evolution algorithm. We used a two-step approach to the fit which allowed us to establish first a subset of 7 parameters ($\lambda$ and $k_p$ for each strain and $\beta$) that shape the lag and exponential phases of growth. Subsequently, we fixed $\beta$ and the $\lambda$s, and fitted the remaining parameters. Details of the fitting procedure are found in the SI, and the results of the fit in Table 1 of the Supplementary text.

**Acknowledgments**

We gratefully acknowledge Laurent Aussel, Dirk Bumann, Sophie Helaine, Jakob Moller Jensen and Fabai Wu for providing the biosensors and fluorescent cell cycle reporters. We thank Parul Singh and Xavier de Bolle for careful reading of the manuscript and fruitful discussions. We are very grateful to the members of the CIRB imaging facility. This work has received support from the program «Investissements d'Avenir » launched by the French Government and implemented by ANR with the references ANR--10--LABX--54 MEMOLIFE and ANR--11--IDEX--0001--02 PSL* Research University, from the ANR with the reference ANR-18-CE35-0007 and the support of the association François Aupetit (AFA).

640 Table S1. Strains

| Name | genotype | description | reference |
|---|---|---|---|
| AIEC LF82 | | | (Glasser *et al.,* 2001) |
| AIEC LF82 Δbla | *ampC* | | Gift from Nicolas Barnich |
| AIEC LF82 Δ*htrA* | *htrA* | | (Bringer *et al.,* 2005) |
| AIEC LFGD1 | AIEC LF82 *Δbla relA::kan* | | This work |
| AIEC LFGD4 | AIEC LF82 *Δbla ydeO::kan* | | This work |
| AIEC LFGD6 | AIEC LF82 *Δbla lon::kan* | | This work |
| AIEC LFGD9 | AIEC LF82 *Δbla recA::kan* | | This work |
| AIEC LFGD11 | AIEC LF82LF82 *Δbla HupA-mcherry-FRT-kan-FRT* | | This work |
| AIEC LFGD13 | AIEC LF82 *Δbla pspA::kan* | | This work |
| AIEC LFGD15 | AIEC LF82 *Δbla soxS::kan* | | This work |
| AIEC LFGD27 | AIEC LF82 *Δbla phoP::kan* | | This work |
| AIEC LFGD30 | AIEC LF82 *Δbla evgA evgS::kan* | | This work |
| AIEC LFGD40 | AIEC LF82 *Δbla evgAS-FRT phoP::kan* | | This work |
| AIEC LFGD41 | AIEC LF82 *Δbla evgAevgS-FRT ydeO::kan* | | This work |
| AIEC LFGD56 | AIEC LF82 *Δbla relA-FRT* | | This work |
| AIEC LFGD57 | AIEC LF82 *Δbla relA-FRT spoT::kan* | | This work |
| AIEC LFGD69 | AIEC LF82 *Δbla lexAind-::kan* | Mutation X-> Y in *lexA* constructed by recombineering | This work |
| AIEC LFGD79 | AIEC LF82 *Δbla dksA::kan* | | This work |

| | | | |
|---|---|---|---|
| AIEC LFER1 | AIEC LF82 *Δbla lexAind-FRT dksA::kan* | | This work |
| AIEC LFER2 | AIEC LF82 *Δbla dksA-FRT recA::kan* | | This work |
| AIEC LFGD86 | AIEC LF82 *Δbla sulA::kan* | | This work |
| AIEC LFGD83 | AIEC LF82 *Δbla ppk-ppX::kan* | | This work |
| AIEC LF82 ΔrpoS | *rpoS::kan* | | Gift from Jakob Moller Jensen (Simonsen *et al.,* 2011) |

641

642

643 Table S2. Plasmids

| name | description | Antibiotic resistance | reference |
|---|---|---|---|
| pKOBEGA | | ampR specR | (Derbise *et al.,* 2003) |
| pAD37 | Matrix vector for recombineering | kanR | (David *et al.,* 2014) |
| pFWZ5 | Para-fts-sfGFP-T::aph | kanR | Gift from Fabai Wu (Wu *et al.,* 2015) |
| pFCcGi | pFP25 P*rpsM-mCherry*, ParaBAD-GFP | ampR | Gift from Sophie Helaine (Helaine *et al.,* 2014) |
| pP*rpsm-mcherry* | pGBM2-P*rpsM-mCherry* | specR | This work |
| pSC101-TIMER bac | | | Gift from Dirk Bumann (Claudi *et al.,* 2014) |
| pom1-GFP | pGBM2-Pro3-GFP | | (Espéli *et al.,* 2001) |

| | | | |
|---|---|---|---|
| pLA42 | pFPV25 PkatG-gfpmut3 | ampR | Gift from Laurent Aussel (Viala *et al.,* 2011; Hébrard *et al.,* 2009) |
| pP1485 | pFPV25 P*asr-gfp* | ampR | Gift from Laurent Aussel (Viala *et al.,* 2011; Hébrard *et al.,* 2009) |
| pmgtC | pFPV25 P*mgtC-gfp* | ampR | Gift from Laurent Aussel (Viala *et al.,* 2011; Hébrard *et al.,* 2009) |
| pSulA-GFP | pZA31MCS-delta Xho P*sulA-GFP* | | (Esnault *et al.,* 2007) |

644

645

646 **References**


647 Amato SM & Brynildsen MP (2015) Persister Heterogeneity Arising from a Single
648 Metabolic Stress. *Curr. Biol. CB* **25:** 2090–2098

649 Amato SM, Fazen CH, Henry TC, Mok WWK, Orman MA, Sandvik EL, Volzing KG &
650 Brynildsen MP (2014) The role of metabolism in bacterial persistence. *Front.*
651 *Microbiol.* **5:** 70

652 Balaban NQ, Merrin J, Chait R, Kowalik L & Leibler S (2004) Bacterial persistence as a
653 phenotypic switch. *Science* **305:** 1622–1625

654 Barnich N, Bringer M-A, Claret L & Darfeuille-Michaud A (2004) Involvement of
655 lipoprotein NlpI in the virulence of adherent invasive Escherichia coli strain LF82
656 isolated from a patient with Crohn's disease. *Infect. Immun.* **72:** 2484–2493

657 Bernier SP, Lebeaux D, DeFrancesco AS, Valomon A, Soubigou G, Coppée J-Y, Ghigo J-M &
658 Beloin C (2013) Starvation, together with the SOS response, mediates high
659 biofilm-specific tolerance to the fluoroquinolone ofloxacin. *PLoS Genet.* **9:**
660 e1003144

661 Bigger J (1944) TREATMENT OF STAPHYLOCOCCAL INFECTIONS WITH PENICILLIN BY
662 INTERMITTENT STERILISATION. *The Lancet* **244:** 497–500

663 den Blaauwen T, Lindqvist A, Löwe J & Nanninga N (2001) Distribution of the
664 Escherichia coli structural maintenance of chromosomes (SMC)-like protein
665 MukB in the cell. *Mol. Microbiol.* **42:** 1179–1188

666 Bringer M-A, Barnich N, Glasser A-L, Bardot O & Darfeuille-Michaud A (2005) HtrA
667 stress protein is involved in intramacrophagic replication of adherent and
668 invasive Escherichia coli strain LF82 isolated from a patient with Crohn's disease.
669 *Infect. Immun.* **73:** 712–721

670 Bringer M-A, Billard E, Glasser A-L, Colombel J-F & Darfeuille-Michaud A (2012)
671 Replication of Crohn's disease-associated AIEC within macrophages is dependent
672 on TNF-α secretion. *Lab. Investig. J. Tech. Methods Pathol.* **92:** 411–419

673 Bringer M-A, Glasser A-L, Tung C-H, Méresse S & Darfeuille-Michaud A (2006) The
674 Crohn's disease-associated adherent-invasive Escherichia coli strain LF82
675 replicates in mature phagolysosomes within J774 macrophages. *Cell. Microbiol.* **8:**
676 471–484

677 Bringer M-A, Rolhion N, Glasser A-L & Darfeuille-Michaud A (2007) The oxidoreductase
678 DsbA plays a key role in the ability of the Crohn's disease-associated adherent-
679 invasive Escherichia coli strain LF82 to resist macrophage killing. *J. Bacteriol.*
680 **189:** 4860–4871

681 Cieza RJ, Hu J, Ross BN, Sbrana E & Torres AG (2015) The IbeA invasin of adherent-
682 invasive Escherichia coli mediates interaction with intestinal epithelia and
683 macrophages. *Infect. Immun.* **83:** 1904–1918

684 Claudi B, Spröte P, Chirkova A, Personnic N, Zankl J, Schürmann N, Schmidt A & Bumann
685 D (2014) Phenotypic variation of Salmonella in host tissues delays eradication by
686 antimicrobial chemotherapy. *Cell* **158:** 722–733

687 Darfeuille-Michaud A, Neut C, Barnich N, Lederman E, Di Martino P, Desreumaux P,
688 Gambiez L, Joly B, Cortot A & Colombel JF (1998) Presence of adherent
689 Escherichia coli strains in ileal mucosa of patients with Crohn's disease.
690 *Gastroenterology* **115:** 1405–1413

691 David A, Demarre G, Muresan L, Paly E, Barre F-X & Possoz C (2014) The two Cis-acting
692 sites, parS1 and oriC1, contribute to the longitudinal organisation of Vibrio
693 cholerae chromosome I. *PLoS Genet.* **10:** e1004448

694 Demarre G, Prudent V & Espéli O (2017) Imaging the Cell Cycle of Pathogen E. coli
695 During Growth in Macrophage. *Methods Mol. Biol. Clifton NJ* **1624:** 227–236

696 Derbise A, Lesic B, Dacheux D, Ghigo JM & Carniel E (2003) A rapid and simple method
697 for inactivating chromosomal genes in Yersinia. *FEMS Immunol. Med. Microbiol.*
698 **38:** 113–116

699 Dörr T, Lewis K & Vulić M (2009) SOS response induces persistence to fluoroquinolones
700 in Escherichia coli. *PLoS Genet.* **5:** e1000760

701 Elhenawy W, Oberc A & Coombes BK (2018) A polymicrobial view of disease potential in
702 Crohn's-associated adherent-invasive E. coli. *Gut Microbes* **9:** 166–174

703 Esnault E, Valens M, Espéli O & Boccard F (2007) Chromosome structuring limits
704 genome plasticity in Escherichia coli. *PLoS Genet.* **3:** e226

705 Espéli O, Moulin L & Boccard F (2001) Transcription attenuation associated with
706 bacterial repetitive extragenic BIME elements. *J. Mol. Biol.* **314:** 375–386

707 Glasser AL, Boudeau J, Barnich N, Perruchot MH, Colombel JF & Darfeuille-Michaud A
708 (2001) Adherent invasive Escherichia coli strains from patients with Crohn's
709 disease survive and replicate within macrophages without inducing host cell
710 death. *Infect. Immun.* **69:** 5529–5537

711 Haeusser DP & Levin PA (2008) The great divide: coordinating cell cycle events during
712 bacterial growth and division. *Curr. Opin. Microbiol.* **11:** 94–99

713 Hajduk IV, Rodrigues CDA & Harry EJ (2016) Connecting the dots of the bacterial cell
714 cycle: Coordinating chromosome replication and segregation with cell division.
715 *Semin. Cell Dev. Biol.* **53:** 2–9

716 Harms A, Fino C, Sørensen MA, Semsey S & Gerdes K (2017) Prophages and Growth
717 Dynamics Confound Experimental Results with Antibiotic-Tolerant Persister
718 Cells. *mBio* **8:**

719 Hébrard M, Viala JPM, Méresse S, Barras F & Aussel L (2009) Redundant hydrogen
720 peroxide scavengers contribute to Salmonella virulence and oxidative stress
721 resistance. *J. Bacteriol.* **191:** 4605–4614

722 Helaine S, Cheverton AM, Watson KG, Faure LM, Matthews SA & Holden DW (2014)
723 Internalization of Salmonella by macrophages induces formation of
724 nonreplicating persisters. *Science* **343:** 204–208

725 Jonas K (2014) To divide or not to divide: control of the bacterial cell cycle by
726 environmental cues. *Curr. Opin. Microbiol.* **18:** 54–60

727 Kim J-S & Wood TK (2017) Tolerant, Growing Cells from Nutrient Shifts Are Not
728 Persister Cells. *mBio* **8:**

729 Kreuzer KN (2013) DNA damage responses in prokaryotes: regulating gene expression,
730 modulating growth patterns, and manipulating replication forks. *Cold Spring*
731 *Harb. Perspect. Biol.* **5:** a012674

732 Lapaquette P, Bringer M-A & Darfeuille-Michaud A (2012) Defects in autophagy favour
733 adherent-invasive Escherichia coli persistence within macrophages leading to
734 increased pro-inflammatory response. *Cell. Microbiol.* **14:** 791–807

735 Lewis K (2010) Persister cells. *Annu. Rev. Microbiol.* **64:** 357–372

736 Manina G, Dhar N & McKinney JD (2015) Stress and host immunity amplify
737 Mycobacterium tuberculosis phenotypic heterogeneity and induce nongrowing
738 metabolically active forms. *Cell Host Microbe* **17:** 32–46

739 Margolin W & Bernander R (2004) How do prokaryotic cells cycle? *Curr. Biol. CB* **14:**
740 R768-770

741 Miquel S, Claret L, Bonnet R, Dorboz I, Barnich N & Darfeuille-Michaud A (2010) Role of
742 decreased levels of Fis histone-like protein in Crohn's disease-associated
743 adherent invasive Escherichia coli LF82 bacteria interacting with intestinal
744 epithelial cells. *J. Bacteriol.* **192:** 1832–1843

745 Mouton JM, Helaine S, Holden DW & Sampson SL (2016) Elucidating population-wide
746 mycobacterial replication dynamics at the single-cell level. *Microbiol. Read. Engl.*
747 **162:** 966–978

748 Radzikowski JL, Vedelaar S, Siegel D, Ortega ÁD, Schmidt A & Heinemann M (2016)
749 Bacterial persistence is an active σS stress response to metabolic flux limitation.
750 *Mol. Syst. Biol.* **12:** 882

751 Rao NN & Kornberg A (1999) Inorganic polyphosphate regulates responses of
752 Escherichia coli to nutritional stringencies, environmental stresses and survival
753 in the stationary phase. *Prog. Mol. Subcell. Biol.* **23:** 183–195

754 Rycroft JA, Gollan B, Grabe GJ, Hall A, Cheverton AM, Larrouy-Maumus G, Hare SA &
755 Helaine S (2018) Activity of acetyltransferase toxins involved in
756 Salmonella persister formation during macrophage infection. *Nat. Commun.* **9:**
757 1993

758 Shan Y, Brown Gandt A, Rowe SE, Deisinger JP, Conlon BP & Lewis K (2017) ATP-
759 Dependent Persister Formation in Escherichia coli. *mBio* **8:**

760 Sharma UK & Chatterji D (2010) Transcriptional switching in Escherichia coli during
761 stress and starvation by modulation of sigma activity. *FEMS Microbiol. Rev.* **34:**
762 646–657

763 Simonsen KT, Nielsen G, Bjerrum JV, Kruse T, Kallipolitis BH & Møller-Jensen J (2011) A
764 role for the RNA chaperone Hfq in controlling adherent-invasive Escherichia coli
765 colonization and virulence. *PloS One* **6:** e16387

766 Tawfik A, Flanagan PK & Campbell BJ (2014) Escherichia coli-host macrophage
767 interactions in the pathogenesis of inflammatory bowel disease. *World J.*
768 *Gastroenterol.* **20:** 8751–8763

769 Verstraeten N, Knapen W, Fauvart M & Michiels J (2016) A Historical Perspective on
770 Bacterial Persistence. *Methods Mol. Biol. Clifton NJ* **1333:** 3–13

771 Viala JPM, Méresse S, Pocachard B, Guilhon A-A, Aussel L & Barras F (2011) Sensing and
772 adaptation to low pH mediated by inducible amino acid decarboxylases in
773 Salmonella. *PloS One* **6:** e22397

774 Wood TK, Knabel SJ & Kwan BW (2013) Bacterial persister cell formation and
775 dormancy. *Appl. Environ. Microbiol.* **79:** 7116–7121

776 Wu F, Van Rijn E, Van Schie BGC, Keymer JE & Dekker C (2015) Multi-color imaging of
777 the bacterial nucleoid and division proteins with blue, orange, and near-infrared
778 fluorescent proteins. *Front. Microbiol.* **6:** 607

779

780

781 **Legend of the figures**

782 **Figure 1. Intracellular LF82 multiplication requires stress responses**. A) Measure of
783 viable and dead AIEC LF82 for 24 h post-infection of THP1 differentiated macrophages.
784 Circles represent average CFU (blue) and Propidium iodide (PI) positive bacteria (black)
785 ± Standard deviation (SD) (dotted lines). To minimize variability this experiment has
786 been performed on one set of THP1 amplified for 8 days before differentiation. B)
787 Analysis by qRT-PCR of the induction of LF82 stress responses at 1 h, 6 h and 24 h P.I. of
788 THP1 macrophages. Values represent the average of two experiments (3 technical
789 replicate each). C) Proportion of viable bacteria at 24 h P.I. of THP1 macrophages in
790 comparison to 1 h. LF82, K12-C600 and LF82 deletion mutants were infected at a MOI of
791 30 which corresponds to 0 - 5 visible bacteria per macrophage at time point 1h (Figure
792 2A). Values represent the average of 3 to 7 experiments ± SD. Horizontal lines indicate
793 viability decrease by 2, 5 and 10 fold compared to WT LF82.

794

795 **Figure 2**. **Intracellular LF82 show heterogeneous stress responses.** A) Imaging of
796 THP1 macrophages infection by LF82-GFP at a MOI of 30. Representative images at 1 h
797 and 24 h. Scale bar is 5 µm B) Imaging of LF82-mCherry stress responses at the single
798 cell level with biosensors. Imaging was performed at 24 h P.I.. LF82-mCherry was
799 transformed with plasmids containing either the *katG* promoter fused to GFP (P*katG*-
800 GFP), the *mgtC* promoter (P*mgt*C-GFP), the *asr* promoter (P*asr*-GFP) or the *sulA*
801 promoter (P*sulA*-GFP). C) Imaging of LF82-mCherry P*asr*GFP and Lamp1 phagolysosome
802 marker E) Measure of the fluorescence intensity of individual LF82-mCherry containing
803 the *katG* promoter fused to GFP at 1 h and 24 h P.I. F) Measure of the fluorescence
804 intensity of individual LF82-mCherry containing the *asr* promoter fused to GFP at 1 h
805 and 24 h P.I. G) LF82 P*sulA*-GFP, LF82 P*katG*GFP, LF82 P*asr*-GFP in LB respectively
806 supplemented with MMC (5µM), with H2O2 (5µM) or switched to pH4.7 1h before
807 imaging. Distribution of the fluorescence of LF82 P*asr*-GFP after 24h post infection in
808 macrophage (from panel B) and after 1 hours of growth in LB buffered at pH4.7.
809 Fluorescence values were expressed as their log2ratio with the average value of the
810 maximum decile (maximum expression). Distributions were compared with a Two-
811 sample Kolmogorov-Smirnov (KS) test.

812

813 **Figure 3. Non-grower LF82 are produced during intracellular growth.** A)
814 Representative image of LF82 containing the fluorescent dilution plasmid (pFC6Gi) at 1
815 h and 24 h post-infection. The frequency of replicative and non-growing LF82 (undiluted
816 GFP) is indicated (N =300). B) Representative image of LF82 containing the TIMER
817 plasmid (pBR-TIMER) at 18 h post-infection. The red arrows points toward the reddest
818 LF82. The frequency of replicative and non-growing LF82 is indicated (N =300). C)
819 Representative images of LF82-mCherry FtsZ-GFP at 1 h and 24 h post-infection.
820 Infections presented in panels A to C were performed with a stationary phase culture of
821 LF82 (O.D. 2). Scale bars are 5 µm. D) Measure of the frequency of LF82 presenting a
822 FtsZ ring in populations growing in LB or within macrophages (N =300).
823
824 **Figure 4. Persisters LF82 are produced during intracellular growth.** A) Measure of
825 the proportion of LF82 that were tolerant to ciprofloxacin (10x MIC) at 1 h or 3 h. LF82
826 were cultivated up to OD 0.3 in LB medium (*in vitro*) or harvested after 1 h or 24 h post
827 infection within macrophages. The challenges exerted on bacteria passaged through
828 macrophages started immediately after macrophage lysis (see experimental
829 procedures). B) Proportion of non-growing LF82 (labeled using the Fluorescent Dilution
830 assay) observed within macrophages (24 h P.I.) following a 6 h ofloxacin treatment. C)
831 Ratio of ciprofloxacin-tolerant versus viable LF82 and K12-C600 bacteria after
832 macrophage infection. Values are averages of 5 experiments. Data were analyzed using a
833 Student's *t* test to determine differences with the proportion of ciprofloxacin-tolerant
834 LF82 at 1 h post-infection, $*P < 0.05$. D) Measure of the proportion of LF82 that were
835 tolerant to ciprofloxacin at 1 h or 3 h with increasing times after macrophage lysis. E)
836 Imaging of the regrowth properties of individual LF82-TIMER bacteria after
837 macrophages lysis. Infections were performed for 20 h and then macrophages were
838 lysed, LF82 spread on to LB agarose pads and immediately imaged at 37°C. TIMER red
839 fluorescence was progressively lost as microcolonies formed. The lysis procedure
840 requires 20 minutes before the first field can be observed (t20 min). F) Measure of the
841 ability of LF82 to form microcolonies as a function of red TIMER fluorescence at t20 min
842 of the experiment are presented in E; areas of microcolonies are expressed in pixels$^2$ ;
843
844 **Figure 5. SOS and stringent responses control LF82 cell cycle in the macrophages.**

845 **.** A) Proportions of LF82, K12-C600 and LF82 deletion mutants that were tolerant to a
846 3h ciprofloxacin challenge following a 1 h or 24 h intracellular period within THP1
847 macrophages. Values represent the average of 3 to 7 experiments. Data were analyzed
848 by using a Student's *t* test to determine differences compared with wild-type LF82. *$P$ <
849 0.05. B) Measure of the proportions of LF82 *lexA ind*, *recA*, *sulA*, *dksA*, *dksA lexAind-*,
850 *dksA recA* mutants that were tolerant to 3 h of cefotaxim challenge after 1 h of
851 macrophage infection. The 3 htime point was below detection limit for the *dksA recA*
852 mutant because of the poor viability of the mutant in macrophages. Cefotaxime only kills
853 growing bacteria; therefore we resuspended LF82 in LB after macrophage lysis. Under
854 these conditions, we did not observe the plateau observed for persisters to
855 ciprofloxacin, suggesting that tolerant rather than persister bacteria were measured. C)
856 Same as in B but with 20 h of macrophage infection. Values represent the average of 3 to
857 7 experiments. Data were analyzed using a Student's *t* test to determine differences
858 compared with wild-type LF82. *$P$ < 0.05. D) Imaging of the FD for the *relA spoT* and
859 *recA* mutants. Imaging at 24 h P.I. at MOI 100. Data represent the % of replicative and
860 non-growing LF82 at 18 h; a total of 300 bacteria were counted. E) Percentage of the
861 LF82 population presenting a high, mid or low level of red TIMER fluorescence at 18 h
862 P.I.. The *recA*, *lexAind-*, *sulA* and *dksA* mutants were tested. F) Live and dead assay
863 performed 1 h and 18 h P.I., in the LF82, LF82*recA*, LF82*lexAind-,* LF82*sulA*,
864 LF82*relAspoT* and LF82*dksA* strains.
865
866 **Figure 6. Kinetics of macrophage infection**. A) Model of infection of THP1
867 macrophages by LF82, describing the processes of net growth, switch to persistence and
868 stress-induced death as explained in the text. Part of the cells that enter the macrophage
869 die at the onset of the infection (t=0). During lag phase ($0<t<\lambda$), death either exactly
870 compensates birth or, in the mutant lacking the stringent response, results in a negative
871 net growth rate $-\delta_1$ . Later in the infection, the net growth rate $\beta$ is positive. Death rate
872 due to stress accumulation (yellow bar) is negligible in the early stages of infection and
873 becomes particularly important at late time points. Bacteria switch to a persistent state
874 at a rate $k_p$ independent of the growth stage. B) Experimental measures of the infection
875 kinetics (CFUs from 5 replicate experiments, circles; persister fractions, stars) collected
876 over 24h for LF82, *E. coli* K12-C600 and LF82 *dksA* and the best fitting parameters
877 (Supplementary text Table 1) of model eq. (1) (Methods). Continuous lines represent

878 total number of bacteria (B+P, continuous line) and persiters (P, dotted line). Vertical
879 lines indicate the duration λ of lag phase. C) Projected changes in infection dynamics for
880 'virtual mutants' LF82*, obtained by varying $k_p$, λ and $d_{max}$ – the parameters that
881 quantitatively differ between LF82 and *E. coli* K12-C600 – around the LF82 best fit
882 solution (black line); colored lines correspond to parameter values within the indicated
883 interval.
884
885 **Figure 7: Dynamic of AIEC LF82 bacterial population during macrophage infection**
886 Upon phagocytosis both replicative (green FtsZ ring) or stationary phase (brown) LF82
887 detect a signal, perhaps nutrient depletion, that led to stringent response activation. This
888 activates a first phenotypic switch toward a non-replicating state (orange) that protects
889 LF82 from dying because of initial stress burst. Among these non-replicating LF82
890 persisters are formed. After this lag phase, a second switch is required to initiate few
891 rounds of replication. The timing and perhaps the frequency of switching from lag phase
892 to replicative phase differentiate LF82 from our control commensal strain. We have not
893 yet identified LF82 specific determinants that allow this switch. Subsequent replication
894 rounds are dependent on the DNA repair machinery. A third switch, linked to the
895 increasing stress or lesions, is turned on in a portion of the replicative population to
896 form new non growers and persisters. The SOS response might also be playing a role at
897 this stage.
898
899
900
901

902 **Legend of the supplementary figures**

903

904 **Supplementary Figure S1**. **Measure of the impact of various stresses on LF82 and**
905 **K12-C600 growth.** A) Growth curves of LF82 and K12-C600 in LB medium at pH 7.4
906 (blue) and in the presence of serine hydroxamate (15 mg/ml), Serine hydroxamate (7
907 mg/ml), EDTA (70 mM) or in LB at pH 4.7 and LB at pH 4.7 in the presence of EDTA (70
908 mM). B) Chemicals or a pH shift were applied at 160 min. B) Same as in A with addition
909 of the antibiotics ciprofloxacin (24 ng/ml) or cefotaxim (800 ng/ml). Data are the mean
910 of 3 technical replicates.

911

912 **Supplementary Figure S2. Intracellular Live and dead assays.** A) Live and dead
913 assay performed in situ on infected macrophages or after macrophage lysis. For in situ
914 experiments a very weak propidium iodide (PI) labeling is observed on putative dead
915 LF82. By contrast strong PI labeling is observed after macrophage lysis. B) Measure of
916 the speed of disappearance after phagocytosis by macrophages of heat-killed LF82. LF82
917 were killed by 15 min incubation at 60°C and subsequently labeled with propidium
918 iodide. Labeled dead LF82 were incubated with macrophage at a MOI of 100. Imaging
919 was performed at 1h, 2h, 3h and 24h post infection. SYTO-9 was used to reveal
920 macrophage and eventual live bacteria. The number of dead LF82 per macrophage was
921 measured at each time points. Data are average of 3 experiments.

922

923 **Supplementary Figure S3**. **Impact of SOS mutations on survival and persistence of**
924 **LF82 strains.** A) Measure of the resistance to Mitomycin C (MMC) of LF82, LF82 *recA*,
925 LF82 *lexAind-*, MG1655, MG1655 *recA* and MG1655 *lexAind-*. B) Measure of the tolerance
926 to cefotaxim of LF82 and LF82 *recA*, LF82 *lexAind-*, LF82 *sulA* grown in LB medium to an
927 OD of 0.2. C) Induction of tolerance to cefotaxim by pretreatment with a subinhibitory
928 dose of ciprofloxacin (24 ng/ml). The data represent the ratio of the number of bacteria
929 that were tolerant to 3 h of cefotaxim in the presence or absence of ciprofloxacin.

930

931 **Supplementary Figure S4**. **Calibration of the fluorescent dilution assay.** A) Growth
932 curve of LF82 pFC6Gi in LB at 37°C. Colored diamonds represent the sampling times
933 analyzed by fluorescence microscopy in the panel B. B) Distribution of GFP fluorescence
934 in the growing population of LF82; GFP fluorescence is expressed as the number of

935 generations (each generation corresponds to a 2-fold decrease in GFP fluorescence
936 compared with the average fluorescence of the fully induced population at t0). C)
937 Distribution of GFP fluorescence in the population of LF82-infecting macrophages.
938 Fluorescence was measured for individual bacteria or small bacterial clusters after
939 macrophage fixation at 1 h, 6 h, 24 h and 48 h post-infection. D) Distribution of the GFP
940 fluorescence in the population of K12-C600 bacteria infecting macrophages.
941 Fluorescence was measured for individual bacteria or small bacterial clusters after
942 macrophage fixation at 1 h and 24 h post-infection.
943
944 **Supplementary Figure S5**. **Calibration of the TIMER assay.** A) Scatter plot of green
945 versus red TIMER fluorescence measured for exponentially growing LF82 (green) and
946 for a culture that had reached stationary phase (red). B) Distribution of the red TIMER
947 fluorescence (Arbitrary fluorescence Intensity, AI) measured for exponentially growing
948 LF82 (green) and stationary phase LF82 (red) at 4 h and 18 h post-infection. Curves
949 represent the normal fit of the data. The middle peak height for exponential and
950 stationary cultures was used to respectively define the fast-mid and mid-slow borders of
951 the boxes.
952
953
954
955

Figure 1

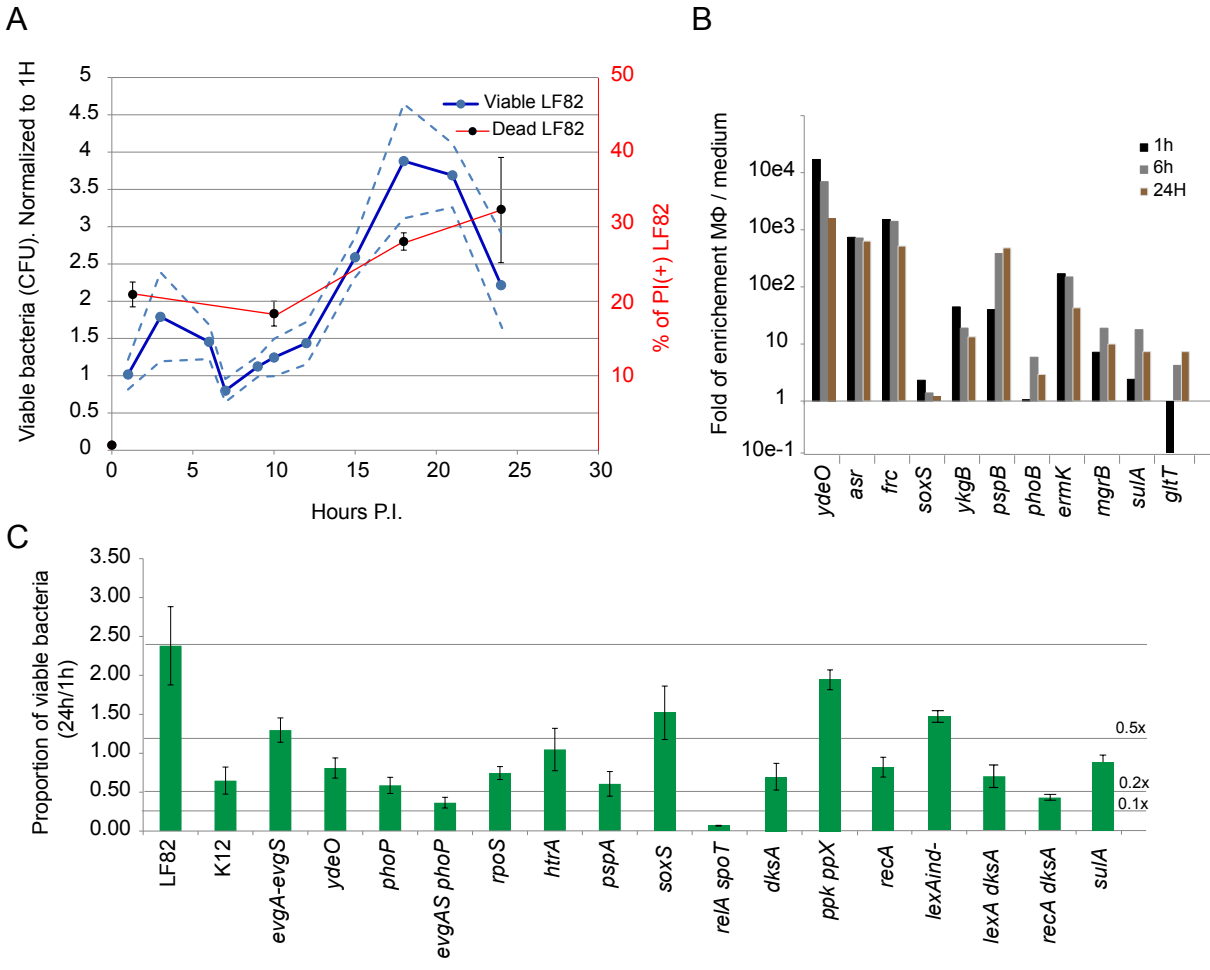
A
Viable bacteria (CFU). Normalized to 1H
% of PI(+) LF82
Viable LF82
Dead LF82
Hours P.I.
B
Fold of enrichement MΦ / medium
1h
6h
24H
ydeO
asr
frc
soxS
ykgB
pspB
phoB
ermK
mgrB
sulA
gltT
C
Proportion of viable bacteria (24h/1h)
0.5x
0.2x
0.1x
LF82
K12
evgA-evgS
ydeO
phoP
evgAS phoP
rpoS
htrA
pspA
soxS
relA spoT
dksA
ppk ppX
recA
lexAind-
lexA dksA
recA dksA
sulA

Figure 2

A

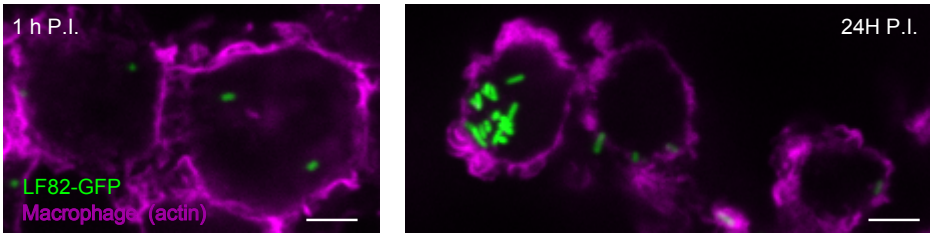


C

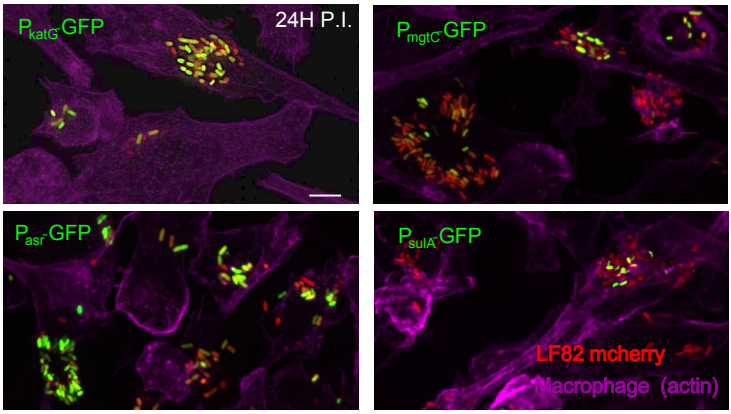


D

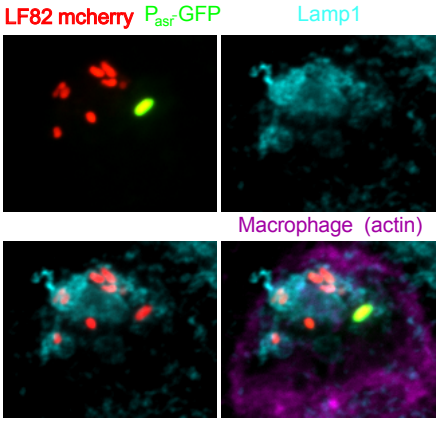


E

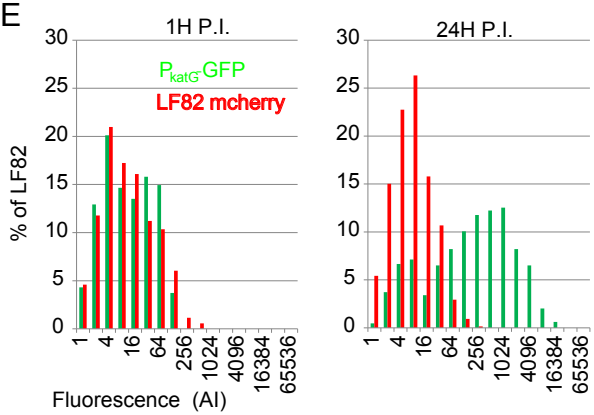


F

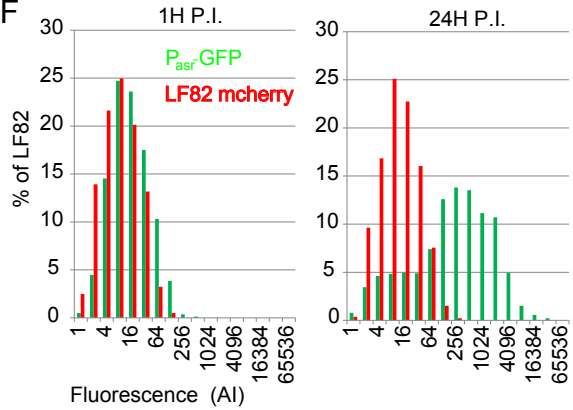


G

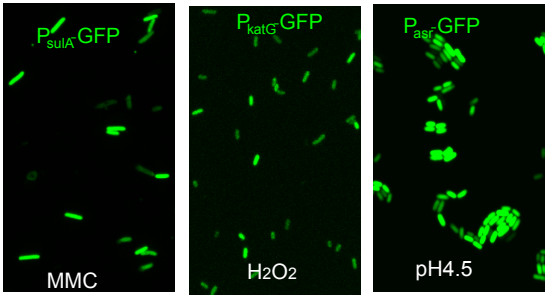


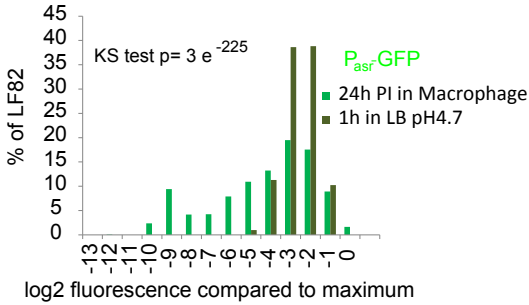

Figure 3

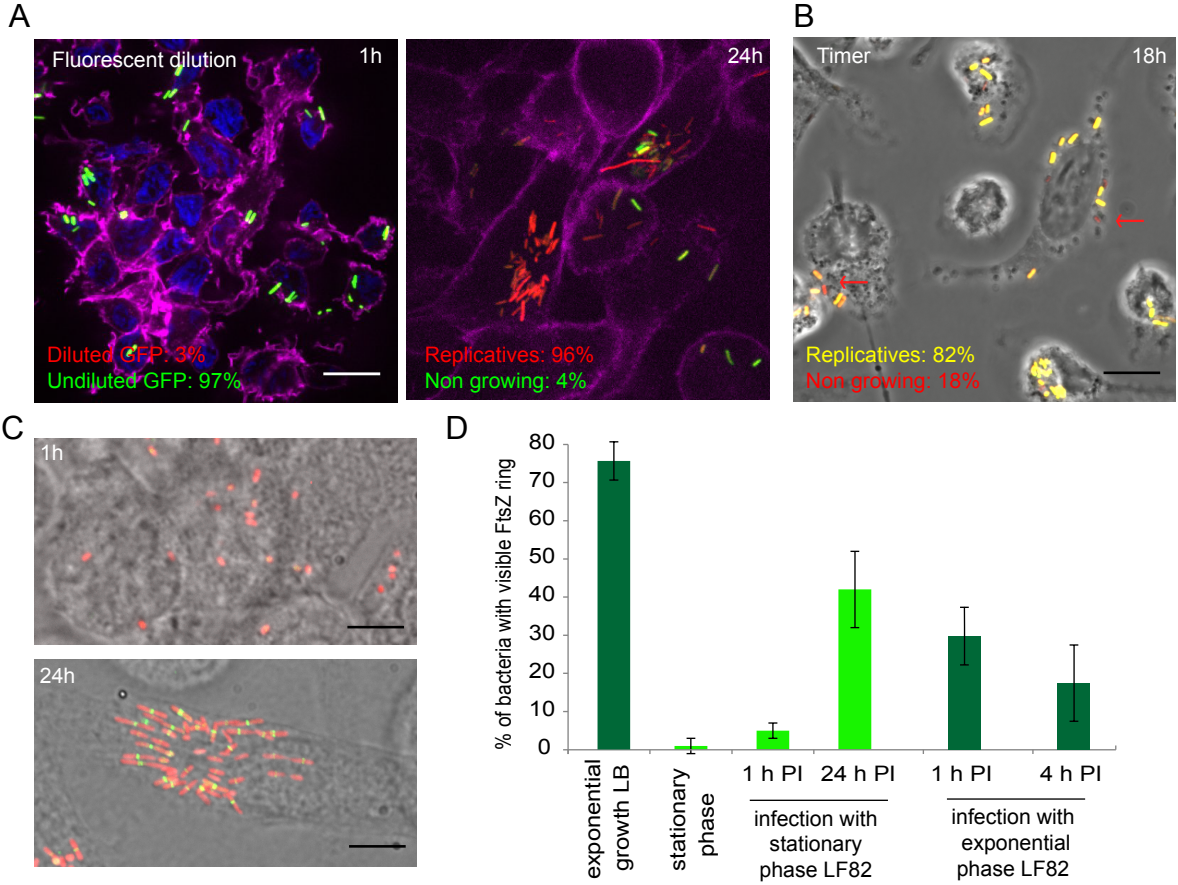
A
Fluorescent dilution
1h
Diluted GFP: 3%
Undiluted GFP: 97%
24h
Replicatives: 96%
Non growing: 4%
B
Timer
18h
Replicatives: 82%
Non growing: 18%
C
1h
24h
D
% of bacteria with visible FtsZ ring
80
70
60
50
40
30
20
10
0
exponential growth LB
stationary phase
1 h PI
24 h PI
infection with stationary phase LF82
1 h PI
4 h PI
infection with exponential phase LF82

Figure 4

A

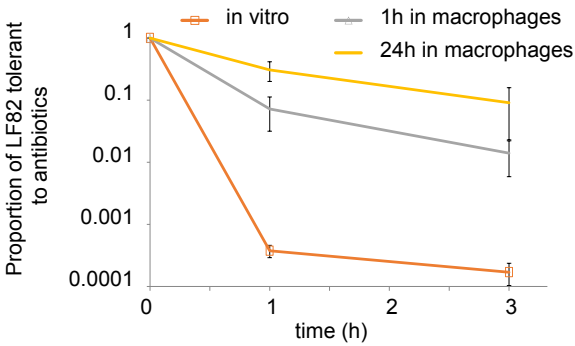


B

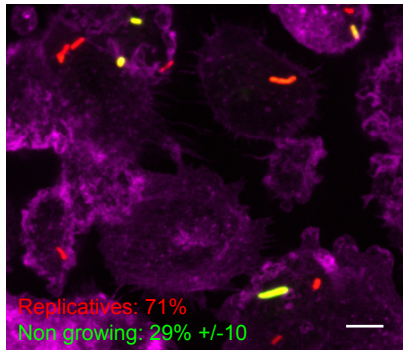


C

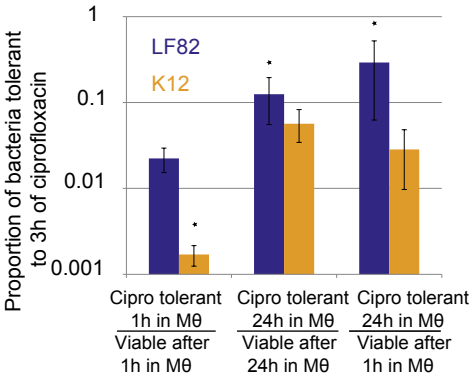


D

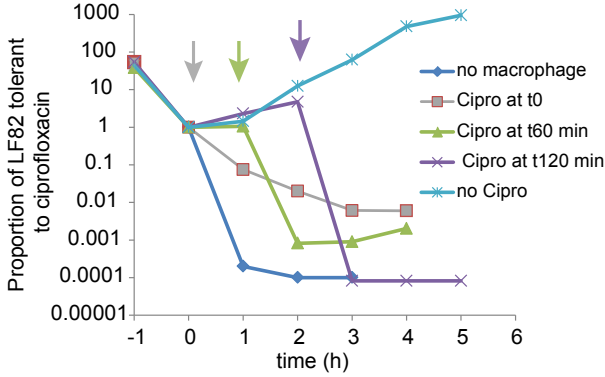


E

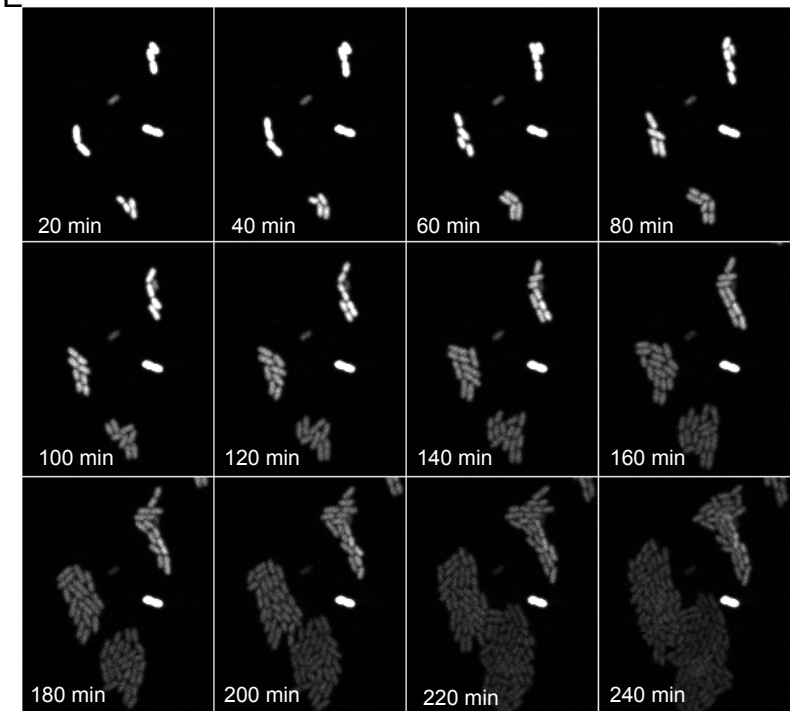


F

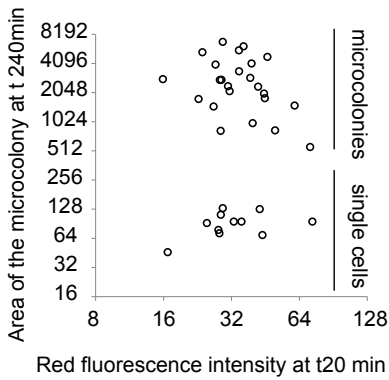

Figure 5

A

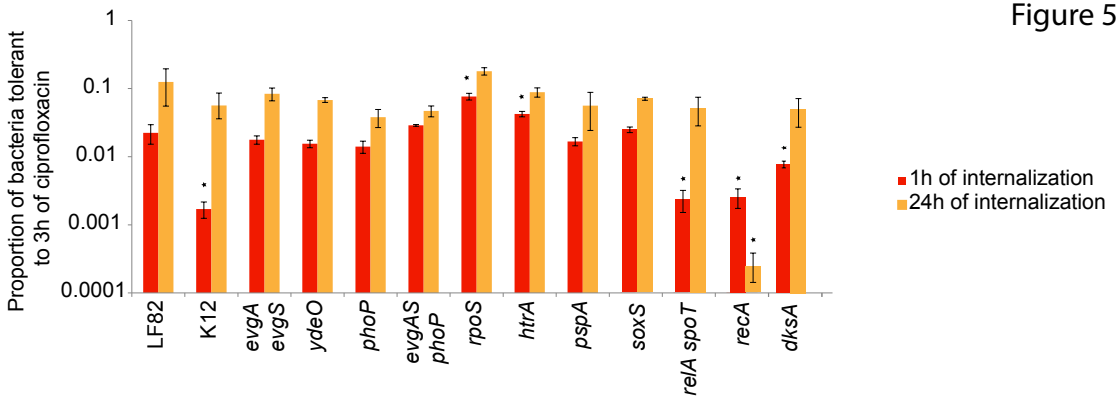


B

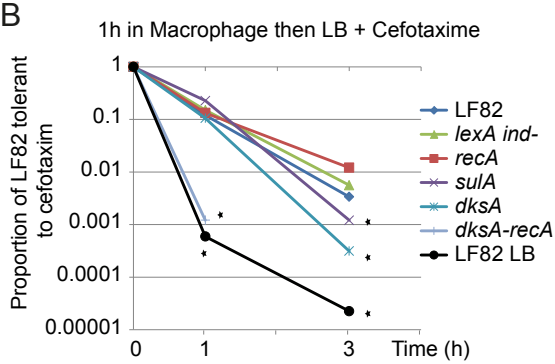


C

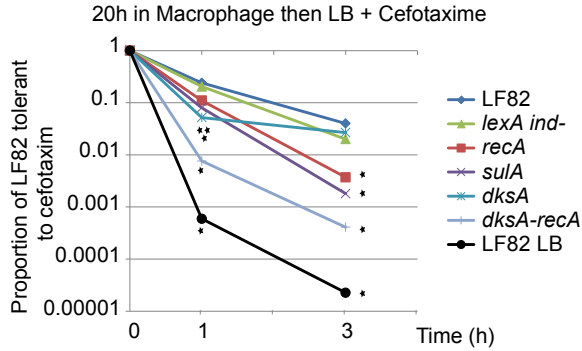


D

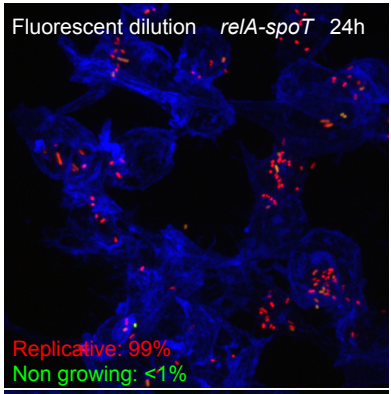


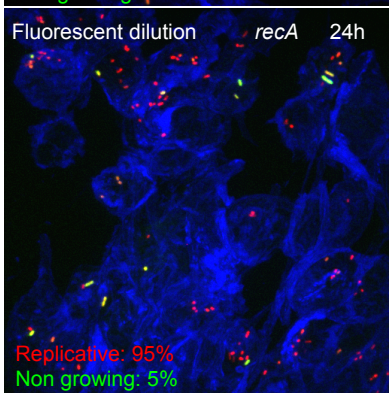


E

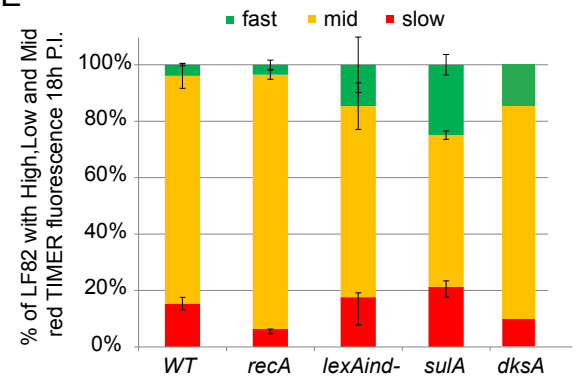


F

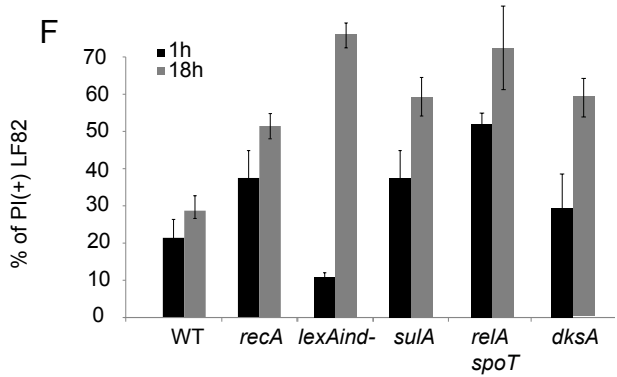

Figure 6

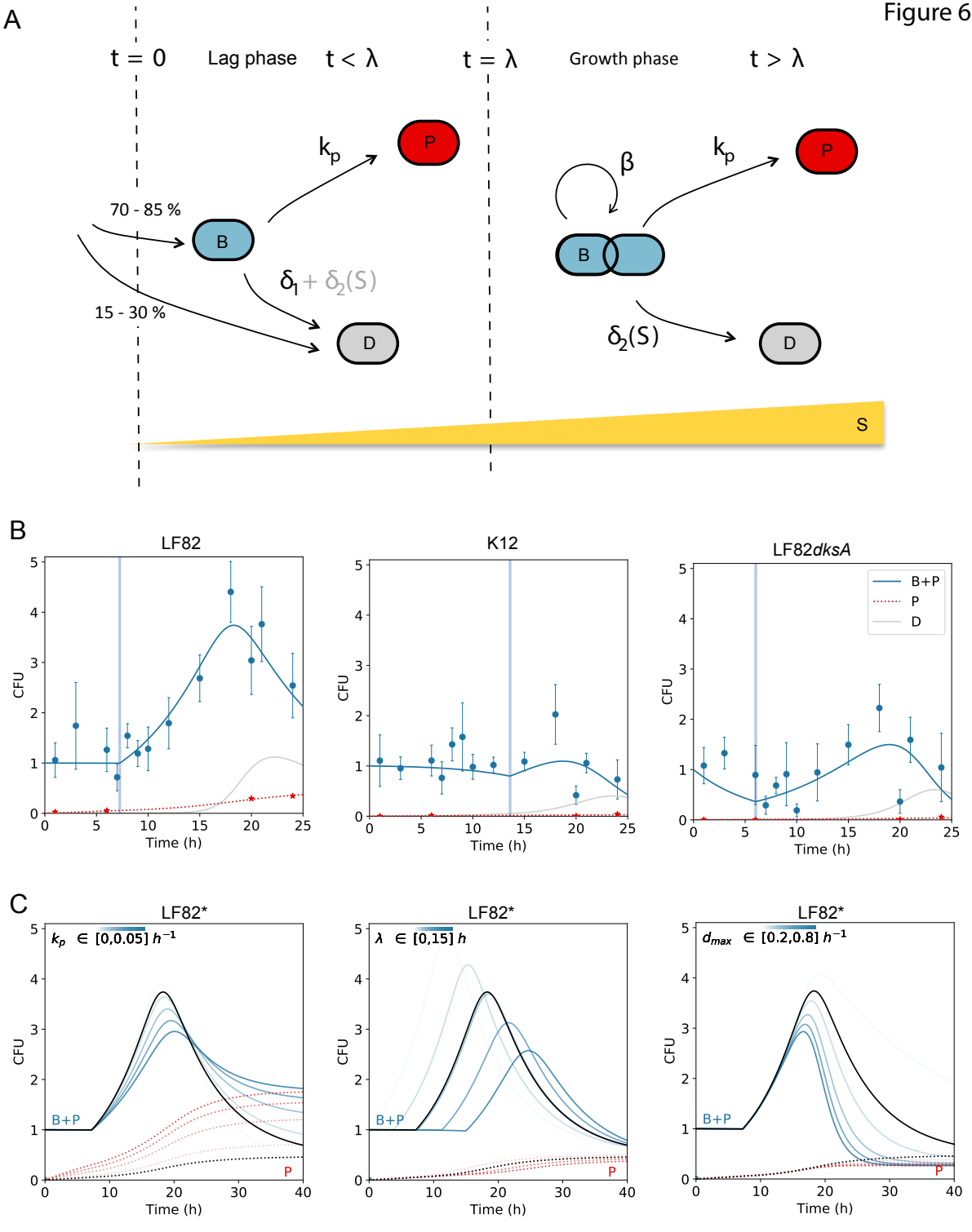
A
t = 0
Lag phase
t < λ
t = λ
Growth phase
t > λ
70 - 85 %
15 - 30 %
B
P
D
$k_p$
$\delta_1 + \delta_2(S)$
β
$\delta_2(S)$
S
B
LF82
K12
LF82dksA
B+P
P
D
CFU
Time (h)
C
LF82*
$k_p \in [0,0.05]\ h^{-1}$
$\lambda \in [0,15]\ h$
$d_{max} \in [0.2,0.8]\ h^{-1}$
B+P
P

Figure 7

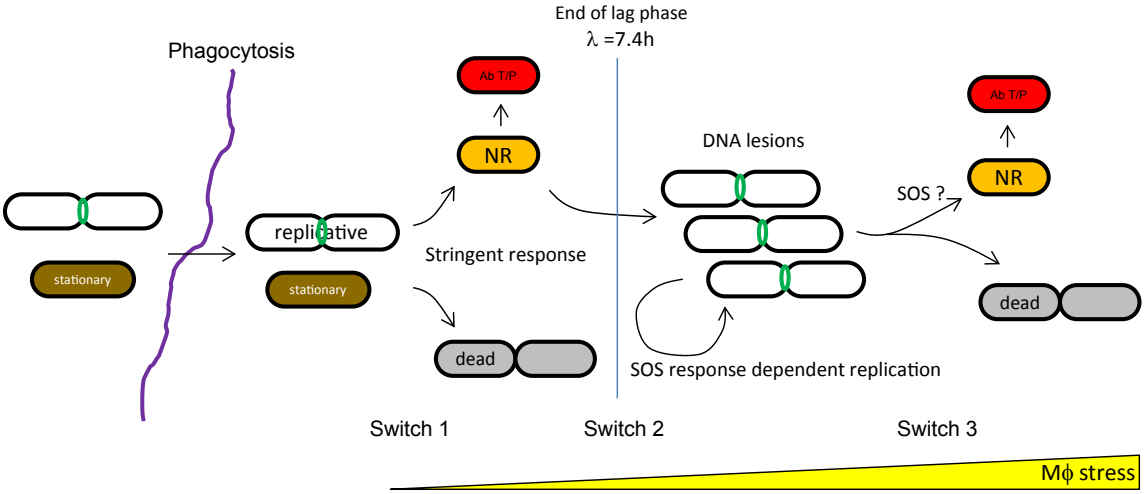
End of lag phase
λ =7.4h
Phagocytosis
Ab T/P
NR
DNA lesions
Ab T/P
NR
SOS ?
stationary
replicative
stationary
Stringent response
dead
dead
SOS response dependent replication
Switch 1
Switch 2
Switch 3
Mϕ stress